


## Research Article

# MicroRNA-26a reduces synovial inflammation and cartilage injury in osteoarthritis of knee joints through impairing the NF- $\kappa$ B signaling pathway

Zhi Zhao<sup>1,2</sup>, Xiu-Song Dai<sup>1,2</sup>, Zhi-Yan Wang<sup>1,2</sup>, Zheng-Qi Bao<sup>1,2</sup> and  Jian-Zhong Guan<sup>1,2</sup>

<sup>1</sup>Department of Orthopedics, The First Affiliated Hospital of Bengbu Medical College, Bengbu 233004, Anhui Province, P.R. China; <sup>2</sup>Anhui Key Laboratory of Tissue Transplantation, Bengbu 233004, Anhui Province, P.R. China

**Correspondence:** Jian-Zhong Guan ([guanjianzhong0531@163.com](mailto:guanjianzhong0531@163.com))



**Objective:** Inflammation is closely implicated in the process of osteoarthritis (OA) and affects disease progression and pain. Herein, the present study explored the effect of microRNA-26a (miR-26a) on the synovial inflammation and cartilage injury in OA, with the involvement with the NF- $\kappa$ B signaling pathway.

**Methods:** Rat models of OA were established by anterior cruciate ligament transection, which were then treated with miR-26a mimics/inhibitors or BMS-345541 (inhibitor of NF- $\kappa$ B pathway). The expression of miR-26a and activator proteins of NF- $\kappa$ B pathway (P-I $\kappa$ B $\alpha$  and P-P65) in synovial tissues was determined. Hematoxylin-eosin (HE) staining was adopted to observe pathological changes of knee joints, synovial tissues, and cartilage of femoral condyle. Terminal deoxynucleotidyl transferase-mediated dUTP nick-end labeling (TUNEL) staining was used to detect the apoptosis of synoviocytes and chondrocytes.

**Results:** Poorly expressed miR-26a and increased protein levels of P-I $\kappa$ B $\alpha$  and P-P65 were identified in synovial tissues of OA rats. Besides, OA rats showed obvious synovial tissue hyperplasia, inflammation and cartilage injury of femoral condyle, as well as increased inflammation and cartilage injury scores, and apoptosis of synoviocytes and chondrocytes. In response to miR-26a mimics, protein levels of P-I $\kappa$ B $\alpha$  and P-P65 were reduced; meanwhile, synovial tissue hyperplasia, inflammation and cartilage injury of femoral condyle were ameliorated, with decreased inflammation and cartilage injury scores, and apoptosis of synoviocytes and chondrocytes.

**Conclusion:** MiR-26a suppressed the activation of the NF- $\kappa$ B signaling pathway, by which mechanism the synovial inflammation and cartilage injury in OA rats were alleviated.

## Introduction

Osteoarthritis (OA) is the most common type of arthritis worldwide, and it is a major contributor to pain and disability among the elderly population [1]. OA mainly afflicts such weight-bearing joints as hips and knees [2]. Additionally, OA is a frequently occurring disorder involving joint damage, progressive aggravation of the joint architecture, and inadequate healing response [3]. OA is characterized by the loss and injury of articular cartilage in the synovial joints and thinning and loss of cartilage is a critical factor in the development and progression of OA [4, 5]. The basis of pathological changes includes all the tissues forming the joint, and OA is involved with inflammation with varying degrees of severity [6]. Multiple researchers emphasized the importance of articular cartilage degeneration and synovitis in OA [7, 8]. Few strategies are available to prevent or treat OA, and multiple molecules and signaling pathways implicated in synovium or cartilage have been studied to understand OA pathogenesis and develop novel therapies [9].

Received: 06 November 2018  
 Revised: 23 February 2019  
 Accepted: 05 March 2019

Accepted Manuscript Online:  
 14 March 2019  
 Version of Record published:  
 09 April 2019

MiRNAs are a class of small, non-protein-coding RNAs functioning as gene regulators, which control target genes and diverse biological pathway [10, 11]. MicroRNA-26a (MiR-26a), located in the non-coding region of CTDSPL gene, regulates inflammation response, cancer pathogenesis, and development through targeting the mRNAs of genes and mediating immune signaling [12–14]. It has been documented that down-regulated miR-26a and miR-26b expressions lead to the pathogenesis of OA through promoting p65 translocation [15]. However, the present study did not clarify how miR-26a and miR-26b functioned in OA and the specific underlying mechanism involved with p65 was largely unknown. A previous study has demonstrated that miR-26a overexpression inhibits NF- $\kappa$ B activity in cardiac fibrosis [16]. Furthermore, miR-26a has also been revealed to suppress pro-inflammatory cytokine production via inactivating NF- $\kappa$ B [17]. Rigoglou et al. [18] proposed that targeted strategies interfering the activation of NF- $\kappa$ B signaling pathway could provide novel potential therapeutic options in the treatment of OA. Specifically, the NF- $\kappa$ B signaling pathway is implicated in the inflammation, angiogenesis, cartilage degradation, and pannus formation in OA and rheumatoid arthritis [19]. Evidence has shown that the expression of miR-26a is dysfunctional in plasma of patients with acute and chronic inflammatory diseases [20]. The up-regulation of hsa-circ-0005105 in OA can promote the degradation of extracellular matrix of chondrocytes through regulating miR-26a [21]. These findings suggest that miR-26a plays an important role in OA. Based on the above conclusions, we treated the OA model rats by injecting miR-26 mimics into the knee joint. The results showed that up-regulation of miR-26a might reduce synovitis and cartilage injury by inhibiting the activation of NF- $\kappa$ B signaling pathway in OA rats. Thus, in the present study, we hypothesized that miR-26a and NF- $\kappa$ B signaling pathway played regulatory roles in OA and their effects were exerted in synovial inflammation and cartilage injury to influence OA.

## Materials and methods

### Experimental animals

Totally, 72 clean and healthy Sprague–Dawley (SD) rats, weighing  $200 \pm 20$  g, including 24 male rats and 24 female rats, were purchased from the Experimental Animal Center (License number: SCXK[Chongqing]2007-0005) of the Third Military Medical University (Chongqing, China). The rats were allowed to acclimatize to environment and housed in a clean animal room, with temperature at  $18\text{--}24^{\circ}\text{C}$ , 12 h light/dark cycle and free access to food and water. All experimental protocols used in the present study were approved by the Ethics Committee for Animal Experimentation of the First Affiliated Hospital of Bengbu Medical College.

### Animal grouping

In order to observe the role of miR-26a in synovitis and cartilage damage of OA rats, we allocated these rats into five groups with eight rats in each group: normal group (normal rats without any treatment), OA group (OA rats without any treatment), negative control (NC) group (OA rats injected with miR-26a NC sequence through knee joint cavity), miR-26a mimics group (OA rats injected with miR-26a mimics through knee joint cavity), and miR-26a inhibitors group (OA rats injected with miR-26a inhibitors through knee joint cavity). In order to further observe whether miR-26a has effect on synovitis and cartilage damage of OA rats by regulating the NF- $\kappa$ B signaling pathway, we allocated the remaining rats into four group ( $n=8$ ), OA group (OA rats without any treatment), NC group (OA rats injected with miR-26a NC sequence through knee joint cavity), BMS-345541 group (OA rats injected with inhibitor of NF- $\kappa$ B signaling pathway, BMS-345541, through knee joint cavity), and miR-26a inhibitors + BMS-345541 group (OA rats injected with miR-26a inhibitors and inhibitor of NF- $\kappa$ B signaling pathway, BMS-345541, through knee joint cavity). MiR-26a NC sequence, miR-26a mimics, and miR-26a inhibitors were purchased from Shanghai GenePharma Co., Ltd. (Pudong District, Shanghai, China). BMS-345541 was purchased from Sigma (Santa Clara, CA, U.S.A.).

### Establishment of OA models in rats

Anterior cruciate ligament (ACL) transection was employed to establish rat models of OA. Except for those in the normal group, the rats were fixed on the operation table in a supine position. A 1 cm incision was made in the medial side of the right knee joint to expose the medial collateral ligament, which was then cut off. The joint capsule was opened to examine whether there was primary lesion in the joint cavity. Then the ACL was transected and the medial meniscus was completely cut off. The incisions were sutured layer by layer, bandaged under sterile conditions, and fixed. Following the operation, antibiotic (ampicillin sodium, Nanjing SenBeiJia Biological Technology Co., Ltd., Nanjing, Jiangsu, China) was administered the next day to prevent infection. 1 week after the operation, rats in the OA group and the normal group were conventionally kept. The other groups were treated separately with the same housing conditions.

## Acquisition of experimental specimen and making of pathological section

On the 28th day of experiment, five rats from each group were collected and killed by cervical dislocation. The right knee joint specimen were taken and observed by the naked eye, the muscles around the knee joint was quickly removed to remove the knee joint. The femoral condylar cartilage was removed by circular incision along the femoral edge of the articular capsule. In addition, the femur and tibial fibula were cut off along the bone surface, the joint capsule was cut longitudinally, and the synovial tissue was separated. Then the cartilage and synovial tissue specimens were stored in liquid nitrogen, which were used for pathological detection and terminal deoxynucleotidyl transferase-mediated dUTP nick-end labeling (TUNEL) staining experiment. The knee joints of remaining SD rats were quickly put into liquid nitrogen for later detection of the expression of miR-26a, P-I  $\kappa$ B $\alpha$ , and P-P65 in cartilage and synovial tissues.

The specimens of the joints were fixed with a sharp knife to form a thick slice of 3–5 mm, fixed in 10% formaldehyde solution, and then put into the ethylene diamine tetraacetic acid (EDTA) for routine decalcification. According to the procedure of an automatic dehydrator, the specimens were dehydrated with 70% ethanol, 80% ethanol, 90% ethanol, 95% ethanol I, 95% ethanol II, n-butanol, anhydrous ethanol I and anhydrous ethanol II, each for 2 h, cleared with xylene II for 2 h, embedded with paraffin I and paraffin II, each for 2 h (60–62°C). After conventional paraffin embedding, the sharp blade was used to keep a 4  $\mu$ m thick tissue slice, and the tissue slice was automatically dried in the whole machine, and then stored at room temperature, to be used.

## Hematoxylin-eosin (HE) staining

No less than three slices of synovial and cartilage tissues were taken from each rat in each group. Paraffin sections were dewaxed and hydrated. The pathological changes of synovial and cartilage tissues of each group were analyzed by hematoxylin-eosin (HE) staining under a light microscope. The HE staining of femoral condylar cartilage was observed and scored by two technical experimenters who were not familiar with the study under a microscope. Three visual fields were selected for each picture. Mankin scores were assessed for articular cartilage by the assigned experimenter. The 0–2 scores represent normal cartilage; 3–5 scores represent fibrosis on the surface of cartilage; 6–7 scores represent medium cartilage injury; 8–10 scores represent severe cartilage injury; above 10 scores represent complete loss of cartilage [22]. Three fields of view were selected for synovial tissues, the results were observed and scored by two technical experimenters who were not familiar with the study under a microscope, which were then scored and graded for synovial inflammation: 0–1 score represents normal synovial tissue and level 0; 2–3 scores represent mild synovitis and level 1; 4–6 scores represent medium synovitis and level 2; 7–9 scores represent severe synovitis and level 3 [23, 24].

## TUNEL assay

The paraffin-embedded sections of articular synovial tissues and cartilage tissues of knee joints were collected to perform TUNEL staining. Along the synovial tissue band and cartilage tissue band, the number of apoptotic cells was counted ( $\times 200$ ). A total of ten fields were counted, followed by recording and calculating the mean number of apoptotic cells in each field. The apoptotic synoviocytes and chondrocytes were brown yellow in color. Apoptotic index (AI) = (number of apoptotic cells/total cell number)  $\times$  100%.

## Reverse transcription quantitative PCR (RT-qPCR)

On the 28th day of experiment, Trizol method (Invitrogen, Carlsbad, CA, U.S.A.) was adopted to extract total RNA of half of synovial tissues of knee joints from the remaining three rats of each group. The ultraviolet analysis and formaldehyde gel electrophoresis were employed to confirm the high quality of RNA. Then 1  $\mu$ g RNA was collected and avian myeloblastosis virus (AMV) reverse transcriptases were used for reverse transcription to obtain cDNA. The primers of PCR were designed and synthesized by Invitrogen (Carlsbad, CA, U.S.A.) (Table 1), with glyceraldehyde-3-phosphate dehydrogenase (GAPDH) as an internal reference. The amplification conditions were pre-denaturation (94°C) for 5 min, denaturation (94°C) for 40 s, and followed by annealing for 40 s under 60°C and DNA strands extension for 1 min at 72°C; this protocol ran for 40 cycles, followed by extension for 10 min at 72°C. The PCR products were treated with agarose gel electrophoresis. Threshold value was manually selected at an inflection point of all the parallel rising logarithmic amplification curves, and the threshold cycle ( $C_t$ ) value of each reaction tube was recorded. The data were analyzed by  $2^{-\Delta\Delta C_t}$ , which represents the multiple proportion of gene expression of the experimental group to the control group. The formula was  $\Delta\Delta C_t = [\Delta C_{t \text{ target gene}} - \Delta C_{t \text{ reference gene}}]_{\text{experimental group}} - [\Delta C_{t \text{ target gene}} - \Delta C_{t \text{ reference gene}}]_{\text{control group}}$ . The experiment was conducted in triplicate with mean value calculated.

**Table 1** Primer sequences for RT-qPCR

Gene	Sequence
miR-26a	F: 5'-GGATCCGCAGAACTCCAGAGA-3' R: 5'-TTGGAGGAAAGACGATTTCCGT-3'
GAPDH	F: 5'-ACGGCAAGTTCAACGGCACAG-3' R: 5'-GACGCCAGTAGACTCCACGACA-3'

Note: F, forward; R, reverse.

## Western blot assay

The protein of half of synovial tissues of knee joints from the remaining three rats of each group was extracted. The protein concentration was determined according to the bicinchoninic acid (BCA) protein assay kit (Wuhan Boster Biological Technology Co., Ltd., Wuhan, Hubei, China). The extracted protein added with uploading buffer was boiled at 95°C for 10 min, with 30 µg for each well. Subsequently, 10% PAGE (Wuhan Boster Biological Technology Co., Ltd., Wuhan, Hubei, China) was employed to separate proteins, with electrophoresis voltage 80 V transferring to 120 V by wet transfer method. The proteins were transferred onto polyvinylidene fluoride (PVDF) membranes with transferring voltage of 100 mV for 45–70 min. The membranes were blocked with 5% BSA for 1 h. Primary antibodies of P-IκBα (1: 1000, 9246, Cell Signaling Technology, Beverly, MA, U.S.A.), P-P65 (1: 1000, 3036, Cell Signaling Technology, Beverly, MA, U.S.A.), and β-actin (1: 1000, 3700, Cell Signaling Technology, Beverly, MA, U.S.A.) were added and incubated at 4°C overnight, followed by washing three times (5 min per wash) with Tris-buffered saline with Tween 20 (TBST). Corresponding secondary antibodies (Shanghai Miaotong Biotechnology Co., Ltd., Shanghai, China) were added and incubated for 1 h. The membranes were washed for three times with 5 min for each time. Chemiluminescence reagents were employed to develop images. β-actin was considered as an internal reference. The images of the gels were captured in a Bio-Rad Gel Doc EZ Imager (Bio-Rad, Hercules, CA, U.S.A.). The gray values of target protein bands were analyzed by ImageJ software (National Institutes of Health, Bethesda, MA, U.S.A.). The experiment was conducted in triplicate with mean value calculated.

## Statistical analysis

SPSS 21.0 (IBM Corp, Armonk, NY, U.S.A.) was employed to analyze data in the present study. Measurement data are expressed by mean ± standard deviation. Normally distributed measurement data between two groups were analyzed by the *t* test. Comparison among multiple groups was analyzed by one-way analysis of variance. Pairwise comparison was conducted by the least significant difference (LSD) *t* test. Two-sided *P*-values <0.05 were considered to indicate statistically significant differences.

## Results

### MiR-26a is expressed at a low level in synovial tissue of knee joints of OA rats

RT-qPCR was used to examine the expression of miR-26a in the synovial tissues of knee joints of rats (Figure 1A). A lower expression of miR-26a was found in the synovial tissues of knee joints of OA rats, as compared with the normal rats (*P*<0.05), suggesting that miR-26a expression is associated with OA.

No significant difference was identified in miR-26a expression in the synovial tissues of knee joints of rats between the OA group and the NC group (*P*>0.05). Compared with the OA group, the miR-26a expression was increased in the miR-26a mimics group and reduced in the miR-26a inhibitors group (both *P*<0.05), indicating that the interference of miR-26a mimics and inhibitors was successful (Figure 1B).

### Observation on the gross specimen of knee joint of rats in each group

In the rats of the normal group, the articular cartilage was transparent, blue and white, articular surface was smooth, lustrous and lustrous, there was no softening focus, and articular edge was neat. Synovial surface of joint was smooth, no obvious joint effusion, synovial hyperemia and hypertrophy were found. In the OA group and the NC group, the rats cartilage surface was rough, which was also presented with mild erosion, occasionally cartilage surface cracks, color darkening, occasionally cartilage defects, no osteophyte formation, different degrees of hyperemia, and adhesion of the membrane and increased secretion of synovial fluid. In the miR-26a mimics group, the cartilage was slightly worn and yellowish, irregular in surface and slightly softened in touch – which lost its original luster – which was



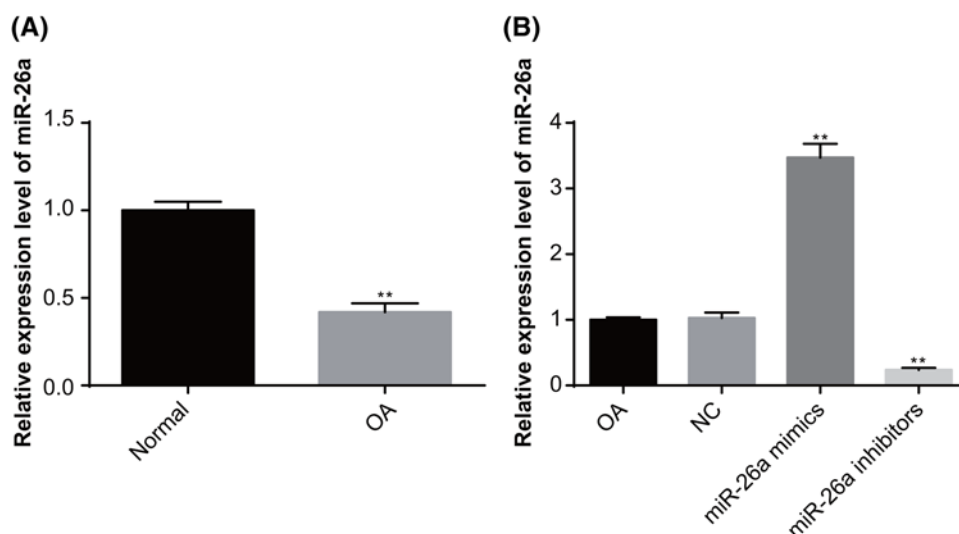


**Figure 1. The expression of miR-26a in the synovial tissues of knee joints of rats detected by RT-qPCR**

Note:  $N=3$ ; (A) the expression of miR-26a in the synovial tissues of knee joints in rats of the OA group and normal group; (B) the expression of miR-26a in the synovial tissues of knee joints in rats following interference of miR-26a mimics and inhibitors; \*\*,  $P<0.01$  compared with the normal group or OA group.

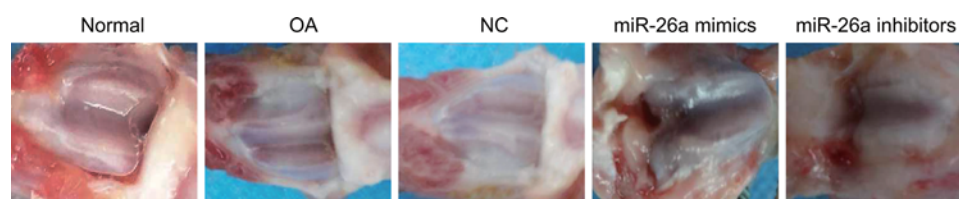


**Figure 2. Gross observation of knee joint of rats in each group**

accompanied by smooth and swollen synovium, mild synovial hyperemia, and a small amount of joint effusion. In the miR-26a inhibitors group, the cartilage surface was worn seriously, ulceration was formed, which was accompanied by partial cartilage defect, subchondral bone exposure, osteophyte formation, synovial hyperplasia and thickening, obvious synovial fibrosis, localized softening foci formation, and decreased synovial fluid volume (Figure 2).

## MIR-26a represses synovial inflammation in knee joint of OA rats

The overall changes of knee joints were observed by a light microscope. In the normal group, the cartilage of knee joint was smooth on the surface, with bright color and regularly arranged chondrocytes. The synovium showed no hyperplasia or fibrosis, and the subchondral bone displayed no hyperplasia or sclerosis. However, the other groups with OA rats all suffered from wear and injury in articular cartilage and synovial hyperplasia, suggesting the successful establishment of OA models. In the OA group and the NC group, obvious articular cartilage injury, synovial hyperplasia, and severe articular wear were observed in the knee joints. Rats in the miR-26a group also had articular cartilage injury, synovial hyperplasia and articular wear in the knee joints, but the severity was reduced as compared with the OA group. The injury in the miR-26a inhibitors group was more severe than the OA group (Figure 3A).

The changes of synovial tissues in knee joints of rats were observed (Figure 3B). The synovial tissues in knee joints of rats in the normal group were normal, without synovial hyperplasia or inflammatory infiltration. Obvious articular synovial tissue hyperplasia and fibroblast-like deposits were found in the knee joints of rats in the OA and the NC groups; meanwhile, plenty of inflammatory infiltration, increased minute vessels, and thickened blood vessel wall were observed. Compared with the OA group, the rats in the miR-26a mimics group showed reduced synovial tissue hyperplasia, inflammatory infiltration, and minute vessels in knee joints, though plenty of inflammatory infiltration still existed. The miR-26a inhibitors group showed notably increased synovial tissue hyperplasia, inflammatory infiltration, and minute vessels in knee joints, when compared with those in the OA group. The inflammation severity in the synovial tissue of knee joints was scored, which are demonstrated in Figure 3C. The rats in the OA and the

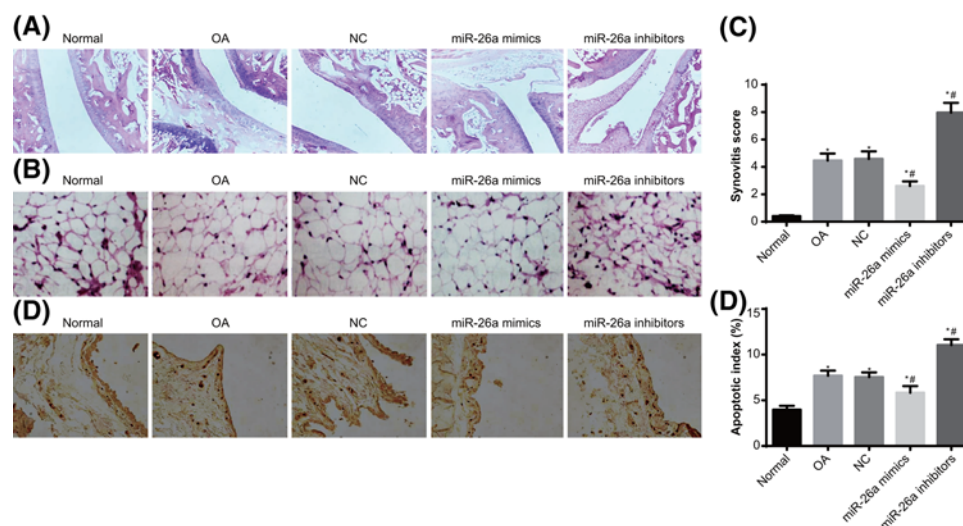


**Figure 3. The pathological changes in the synovium of knee joints of rats**

Note:  $N=5$ ; (A) the pathological changes of knee joints ( $\times 400$ ); (B) the pathological changes of synovial tissues of knee joints ( $\times 200$ ); (C) inflammation scores of synovitis in the knee joints; (D) TUNEL staining was used to observe apoptosis conditions of synoviocytes in knee joints of rats ( $\times 200$ ); (E) quantitative analysis for the AI of synoviocytes in knee joints of rats; \*,  $P<0.05$  compared with the normal group; #,  $P<0.05$  compared with the OA group.

NC groups had medium synovitis, the inflammation scores of which were higher than those in the miR-26a mimics group. The rats in the miR-26a mimics group had mild synovitis in the synovial tissue of knee joints. Severe synovitis in the synovial tissue of knee joints was identified in the miR-26a inhibitors group, with inflammation scores higher than those in the OA and NC groups. No inflammation was found in the synovial tissue of knee joints of normal rats.

TUNEL staining was adopted to observe the apoptosis conditions of synoviocytes in knee joints of rats (Figure 3D,E). Scattered apoptotic synoviocytes were found in the synovial tissues of knee joints of rats in the normal group. Compared with the normal group, the AI of synoviocytes of knee joints in the OA and the NC groups were higher than that in the normal group ( $P<0.05$ ). When compared with the OA and the NC groups, the AI of synoviocytes of knee joints was decreased in the miR-26a mimics group and increased in the miR-26a inhibitors group (all  $P<0.05$ ). These results indicated that overexpressed miR-26a could suppress the synovial inflammatory injury in the knee joints of rats with OA.

## MiR-26a represses cartilage injury of knee joint in OA rats

The pathological changes of femoral condyle cartilage of femoral condyle were observed (Figure 4A). In the normal group, the cartilage of knee joints was intact and smooth on the bright surface, without injuries. The morphology of chondrocytes was normal. The cartilage matrix was uniform in staining intensity and the cartilage structures were clear. In the OA group, the femoral condyle of knee joints showed obvious articular cartilage injuries, with dark color. The cartilage was softened with rough surface, uneven staining intensity, irregularly arranged chondrocytes, and cell aggregation observed. The conditions of cartilage in the NC group were similar to those in the OA group. In the miR-26a mimics group, the staining of cartilage matrix of knee joints was relatively light; the chondrocytes were reduced and tidemark was vague, as compared with the normal group. In the miR-26a inhibitors group, the staining of cartilage matrix of knee joints was uneven, with severely irregularly arranged chondrocytes and plenty of cell aggregation observed. Mankin scoring was adopted to evaluate cartilage injury (Figure 4B). After establishment of rat models of OA, the Mankin scores of cartilage of femoral condyle were all increased (all  $P<0.05$ ). In the miR-26a mimics group, the Mankin scores of cartilage of femoral condyle were lower than those of the OA group ( $P<0.05$ ). The miR-26a inhibitors group had significantly increased Mankin scores of cartilage of femoral condyle as compared with the OA group ( $P<0.05$ ). These results indicated that overexpressed miR-26a reduced cartilage injuries of knee joints of rats with OA.

The apoptosis of femoral condyle chondrocytes in knee joints of rats were evaluated by TUNEL staining (Figure 4C,D). Compared with the normal group, the AI of chondrocytes of knee joints in the OA and NC groups were higher than that in the normal group ( $P<0.05$ ). When compared with the OA and NC groups, the AI of chondrocytes of

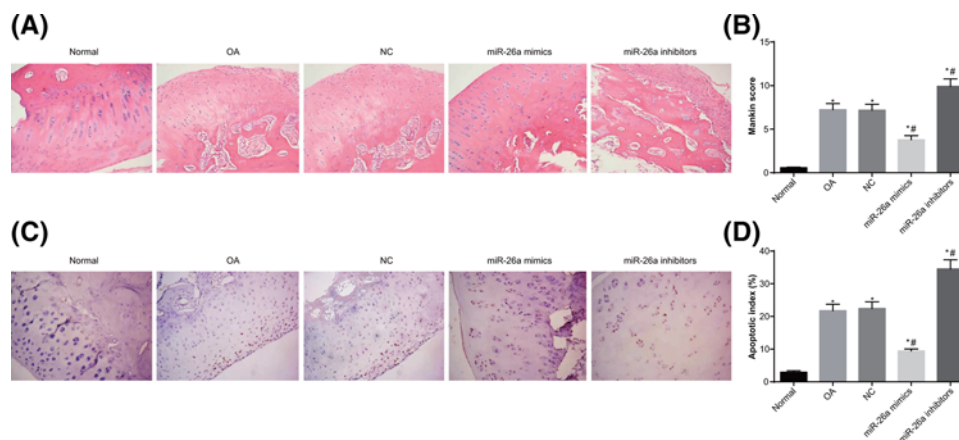


**Figure 4. The pathological changes of cartilage of knee joints in rats**

Note:  $N=5$ ; (A) the pathological changes of femoral condyle cartilage in knee joints ( $\times 200$ ); (B) Mankin scores of femoral condyle cartilage in the knee joints; (C) TUNEL staining was used to observe apoptosis conditions of femoral condyle chondrocytes in knee joints of rats ( $\times 200$ ); (D) quantitative analysis for the AI of femoral condyle chondrocytes in knee joints of rats; \*,  $P < 0.05$  compared with the normal group; #,  $P < 0.05$  compared with the OA group.

knee joints was decreased in the miR-26a mimics group and increased in the miR-26a inhibitors group (all  $P < 0.05$ ). These results indicated that overexpressed miR-26a could suppress the pathological injury in the cartilage of knee joints of rats with OA.

## MiR-26a represses the activation of NF- $\kappa$ B signaling pathway in synovial tissues of knee joints in OA rats

In order to analyze the status of NF- $\kappa$ B signaling pathway in OA and the control of miR-26a on NF- $\kappa$ B signaling pathway, we adopted Western blot assay to examine the protein levels of activating factors of NF- $\kappa$ B signaling pathway (P-I $\kappa$ B $\alpha$  and P-P65) in synovial tissues of knee joints (Figure 5A,B). The OA group had significantly increased protein levels of P-I $\kappa$ B $\alpha$  and P-P65 in synovial tissues of knee joints as compared with the normal group (all  $P < 0.05$ ), suggesting that the NF- $\kappa$ B signaling pathway was aberrantly activated in OA models. No significant differences were identified in protein levels of P-I $\kappa$ B $\alpha$  and P-P65 in synovial tissues of knee joints between the OA group and the NC group (both  $P > 0.05$ ). The protein levels of P-I $\kappa$ B $\alpha$  and P-P65 in synovial tissues of knee joints was reduced in the miR-26a mimics group and increased in the miR-26a inhibitors group, as compared with the OA group (all  $P < 0.05$ ), indicating that miR-26a could inhibit the aberrant activation of NF- $\kappa$ B signaling pathway in OA rats.

BMS-34554 was employed to inhibit the activation of NF- $\kappa$ B signaling pathway in OA rats, under which condition, the protein levels of P-I $\kappa$ B $\alpha$  and P-P65 in synovial tissues of knee joints was reduced. In response to the combined treatment of miR-26a inhibitors and BMS-34554, protein levels of P-I $\kappa$ B $\alpha$  and P-P65 in synovial tissues of knee joints was higher than those in the BMS-34554 group, suggesting that miR-26a regulated the status of NF- $\kappa$ B signaling pathway (Figure 5C,D).

## MiR-26a reduces synovial inflammation in knee joint of OA rats via inhibiting the NF- $\kappa$ B signaling pathway

The NF- $\kappa$ B signaling pathway was aberrantly activated in OA rats. When BMS-34554 was employed to inhibit the activation of NF- $\kappa$ B signaling pathway in OA rats, the synovial hyperplasia, articular cartilage injury and wear were alleviated. The combined treatment of miR-26a inhibitors and BMS-34554 increased the synovial hyperplasia, articular cartilage injury and wear, as compared with the treatment of BMS-34554; while no differences were found as compared with the OA and the NC groups (Figure 6A).

The pathological changes of synovial tissues of knee joints were observed (Figure 6B,C). Compared with the OA and the NC groups, the BMS-34554 group showed reduced synovial tissue hyperplasia, inflammatory infiltration, and minute vessels in knee joints. Compared with the BMS-34554 group, the miR-26a inhibitors + BMS-34554 group had aggravated synovial tissue hyperplasia, inflammatory infiltration and minute vessels in knee joints, represented by increased inflammation scores ( $P < 0.05$ ).

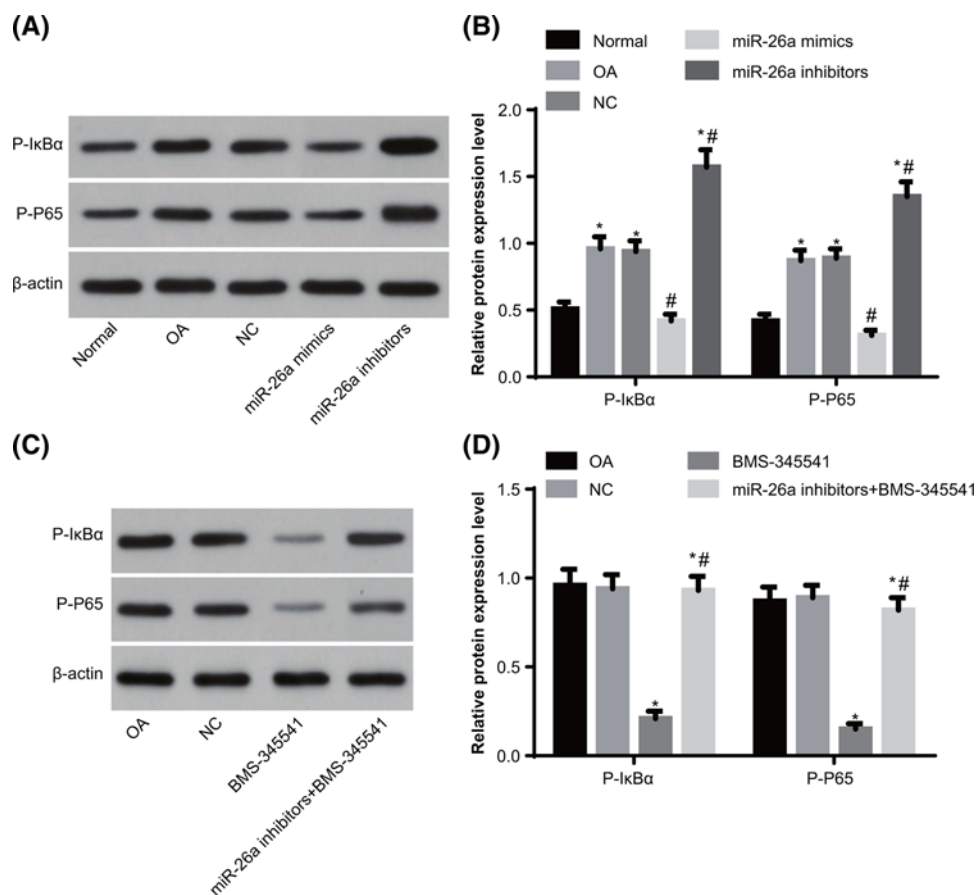


**Figure 5. The status of NF-κB signaling pathway in the synovial tissues of knee joints of rats**

Note:  $N=3$ ; **(A)** Western blot assay was used to evaluate the protein bands of P-IκBα and P-P65 with up-regulation or down-regulation of miR-26a in synovial tissues of knee joints; **(B)** quantitative analysis for the protein levels of P-IκBα and P-P65 with up-regulation or down-regulation of miR-26a in synovial tissues of knee joints; **(C)** Western blot assay was used to evaluate the protein bands of P-IκBα and P-P65 with inhibited NF-κB signaling pathway in synovial tissues of knee joints; **(D)** quantitative analysis for the protein levels of P-IκBα and P-P65 with inhibited NF-κB signaling pathway in synovial tissues of knee joints; \*,  $P<0.05$  compared with the normal group or OA group; #,  $P<0.05$  compared with the OA group or BMS-34554 group.

TUNEL staining was used to evaluate apoptosis of synoviocytes in knee joints (Figure 6D,E). The AI of synoviocytes was higher in the BMS-34554 group than those in the OA and NC groups (both  $P<0.05$ ). Compared with the OA and NC groups, the AI of synoviocytes was not different in the miR-26a inhibitors + BMS-345541 group ( $P>0.05$ ). These findings implied that miR-26a could reduce synovial inflammation in knee joint of OA rats via inhibiting NF-κB signaling pathway.

## MiR-26a reduces cartilage injury in knee joint of OA rats via inhibiting the NF-κB signaling pathway

Obvious articular cartilage injuries were observed in the femoral condyle of knee joints of rats in the OA and NC groups. In comparison to the OA and NC groups, the BMS-34554 group displayed relatively light staining of the femoral condyle cartilage matrix in the knee joints, with relatively mild cartilage injury and reduced Mankin scores (all  $P<0.05$ ). In the miR-26a inhibitors + BMS-345541 group, the staining of the femoral condyle cartilage matrix in the knee joints was uneven, with irregularly arranged chondrocytes; the cartilage injury was similar to the OA and NC groups; Mankin scores were increased as compared with the BMS-345541 group ( $P<0.05$ ) (Figure 7A,B).

Meanwhile, TUNEL staining was used to observe the apoptosis of chondrocytes in knee joints of rats (Figure 7C,D). The AI of chondrocytes in knee joints of the BMS-345541 group was lower than those in the OA and NC groups ( $P<0.05$ ). Compared with the BMS-345541 group, the miR-26a inhibitors + BMS-345541 group showed increased AI



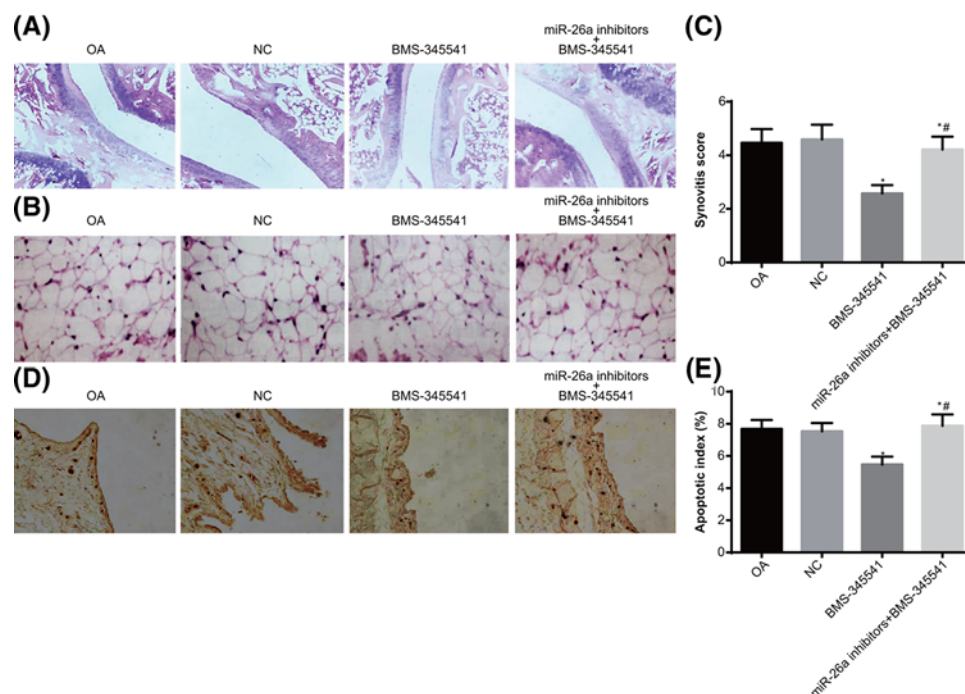


**Figure 6. The pathological changes in the synovium of knee joints of rats**

Note:  $N=5$ ; (A) the pathological changes of knee joints ( $\times 400$ ); (B) the pathological changes of synovial tissues of knee joints ( $\times 200$ ); (C) inflammation scores of synovitis in the knee joints; (D) TUNEL staining was used to observe apoptosis conditions of synoviocytes in knee joints of rats ( $\times 200$ ); (E) quantitative analysis for the AI of synoviocytes in knee joints of rats; \*,  $P<0.05$  compared with the OA group; #,  $P<0.05$  compared with the BMS-34554 group.

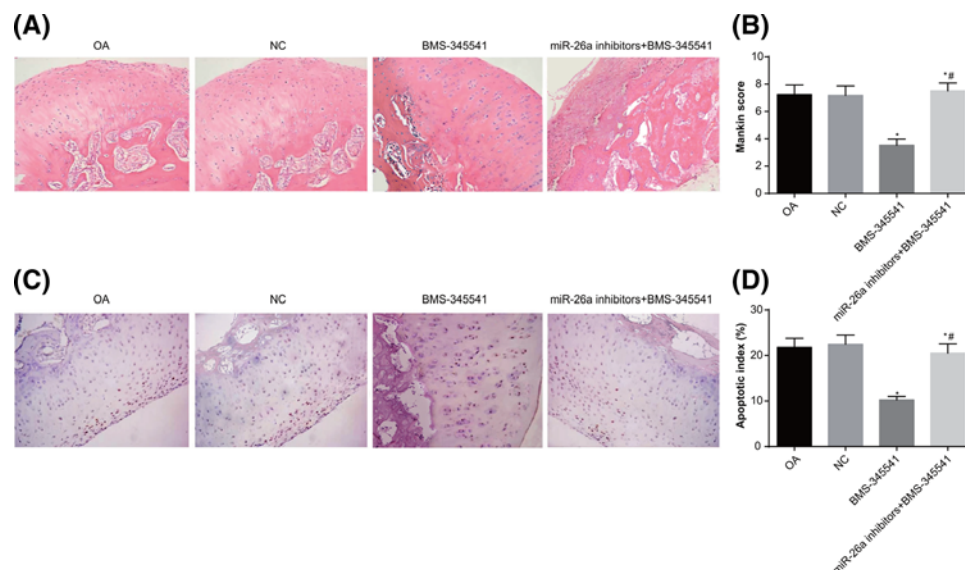


**Figure 7. The pathological changes of cartilage of knee joints in rats**

Note:  $N=5$ ; (A) the pathological changes of femoral condyle cartilage in knee joints ( $\times 200$ ); (B) Mankin scores of femoral condyle cartilage in the knee joints; (C) TUNEL staining was used to observe apoptosis conditions of femoral condyle chondrocytes in knee joints of rats ( $\times 200$ ); (D) quantitative analysis for the AI of femoral condyle chondrocytes in knee joints of rats; \*,  $P<0.05$  compared with the OA group; #,  $P<0.05$  compared with the BMS-34554 group.

of chondrocytes in knee joints ( $P < 0.05$ ). These findings implied that down-regulation of miR-26a expression could deteriorate the pathological injuries of cartilage in knee joints; whereas, blockade of the NF- $\kappa$ B signaling pathway could reverse the effect of miR-26a inhibitors.

## Discussion

OA, common in older adults, is a highly prevalent, chronic, degenerative condition inflicting joint inflammation, pain and even disability on patients [25–27]. It is reported that age is an essential contributing factor for the poor cartilage repair following injury, and also, to the development of OA [28,29]. Interestingly, miR-26a has been reported to be a candidate biomarker for the diagnosis and treatment of systemic juvenile idiopathic arthritis [30]. Moreover, the role of NF- $\kappa$ B activity has been highlighted as a new imaging biomarker in pain sensitivity in mouse models of OA [31]. Therefore, we investigated the relationship of miR-26a and the NF- $\kappa$ B signaling pathway in rat models of OA in knee joints, as well as their effect on the synovial inflammation and cartilage injury.

The OA models of knee joints were established in rats by ACL transection. In the synovial tissues of OA rats, obvious synovial tissue hyperplasia, inflammation, and cartilage injury of femoral condyle were observed; meanwhile, we found increased inflammation and cartilage injury scores and apoptosis of synoviocytes and chondrocytes. Benito et al. [32] stated that elevated mononuclear cell infiltration and overexpression of regulators of inflammation were identified in OA. The loss and degeneration of cartilage matrix are associated with OA progression [33]. Articular chondrocytes exhibit a decline in proliferative capacity while producing pro-inflammatory regulators and matrix degrading enzymes in the process of OA [34]. Furthermore, blood vessel formation is accompanied by secretion of pro-apoptotic cytokines contributing to chondrocytic death, and newly formed vasculature in the synovial membrane leads to promotion of an inflammatory process [35]. Notably, the detection of RT-qPCR demonstrated a low expression level of miR-26a in synovial tissues of OA rats. In response to miR-26a mimics, the synovial inflammation and cartilage injury were ameliorated. The sponging of miR-26a induced by circRNA hsa\_circ.0005105 enhances chondrocyte extracellular matrix degradation [21]. Etich et al. [36] argues that her data support the view that dysregulation of miR-26a expression led to extracellular matrix changes in cartilage diseases.

Corroborating with our study, another study indicated that the low expression level of miR-26a was associated with increased chronic inflammation in the chondrocytes in obese mouse model; whereas, up-regulated miR-26a expression attenuated activation of NF- $\kappa$ B and secretion of pro-inflammatory cytokines in articular chondrocytes [17]. Based on the Western blot analysis, increased protein levels of P-I $\kappa$ B $\alpha$  and P-P65 were identified in synovial tissues of OA rats, suggesting the aberrant activation of the NF- $\kappa$ B signaling pathway. Upon activation, the NF- $\kappa$ B signaling pathway triggers the expression of genes inducing destruction of articular joints, resulting in OA occurrence and progression [18]. When the NF- $\kappa$ B dependent genes were depleted by overexpression of sirtuin 6, the OA development was inhibited through decreasing the inflammatory response and the senescence of chondrocytes [37]. In addition, by suppressing NF- $\kappa$ B and MAPKs signaling pathways, thymoquinone repressed the IL-1 $\beta$ -induced inflammation in chondrocytes of OA [38]. The high activation of NF- $\kappa$ B signaling pathway in synovial fibroblasts causes the majority of the synovial inflammation associated with rheumatoid arthritis [39]. Vasoactive intestinal peptide, as an anti-inflammatory and anti-rheumatic agent, ameliorates synovial cell functions of collagen-induced arthritis rats through down-regulation of the activity and expression of NF- $\kappa$ B [40].

In order to analyze the status of NF- $\kappa$ B signaling pathway in OA and the control of miR-26a on NF- $\kappa$ B signaling pathway, we adopted Western blot assay to examine the protein levels of activating factors of NF- $\kappa$ B signaling pathway (P-I $\kappa$ B $\alpha$  and P-P65) in synovial tissues of knee joints. The results indicated that miR-26a repressed the activation of NF- $\kappa$ B signaling pathway in synovial tissues of knee joints in OA rats. It has been reported that the activation of NF- $\kappa$ B was suppressed by overexpression of miR-26a [16]. In atherosclerosis, miR-26a overexpression suppressed inflammatory response through suppressing the activation of the NF- $\kappa$ B signaling pathway [41]. Besides, in obesity-related chronic inflammation in chondrocytes, a reciprocal inhibition between miR-26a and NF- $\kappa$ B downstream of non-esterified fatty acid signaling has been demonstrated [17].

Based on observations and evaluations made during the study it was suggested that miR-26a suppressed the activation of the NF- $\kappa$ B signaling pathway in the synovial tissues of knee joints in OA rats, in response to which, the synovial inflammation and cartilage injury in OA rats were alleviated. MiR-26a may act as a novel prognostic marker and new therapeutic target for OA in knee joints. Further work should be performed to obtain more information about the specific mechanisms, and to explore the clinical value for OA.

## Acknowledgements

The authors would like to express thanks to the reviewers for critical comments on the present study.

## Competing interests

The authors declare that there are no competing interests associated with the manuscript.

## Funding

The authors declare that there are no sources of funding to be acknowledged.

## Author contribution

Z.Z. and J.-Z.G. designed the study and are the guarantors of integrity of the entire study. X.-S.D. and Z.-Y.W. overlooked the experimental studies. Z.-Q.B. edited the manuscript.

## Abbreviations

ACL, anterior cruciate ligament; AI, apoptotic index; C<sub>t</sub>, threshold cycle; GAPDH, glyceraldehyde-3-phosphate dehydrogenase; HE, hematoxylin-eosin; miR-26a, microRNA-26a; NC, negative control; OA, osteoarthritis; RT-qPCR, Reverse transcription quantitative PCR; SD, Sprague-Dawley; TUNEL, terminal deoxynucleotidyl transferase-mediated dUTP nick-end labeling.

## References

- Arc, O.C. et al. (2012) Identification of new susceptibility loci for osteoarthritis (arcOGEN): a genome-wide association study. *Lancet* **380**, 815–823, [https://doi.org/10.1016/S0140-6736\(12\)60681-3](https://doi.org/10.1016/S0140-6736(12)60681-3)
- Zhen, G. et al. (2013) Inhibition of TGF-beta signaling in mesenchymal stem cells of subchondral bone attenuates osteoarthritis. *Nat. Med.* **19**, 704–712, <https://doi.org/10.1038/nm.3143>
- Andia, I. and Maffulli, N. (2013) Platelet-rich plasma for managing pain and inflammation in osteoarthritis. *Nat. Rev. Rheumatol.* **9**, 721–730, <https://doi.org/10.1038/nrrheum.2013.141>
- Wang, Q. et al. (2011) Identification of a central role for complement in osteoarthritis. *Nat. Med.* **17**, 1674–1679, <https://doi.org/10.1038/nm.2543>
- Litwic, A. et al. (2013) Epidemiology and burden of osteoarthritis. *Br. Med. Bull.* **105**, 185–199, <https://doi.org/10.1093/bmb/lds038>
- Wojdasiewicz, P., Poniatowski, L.A. and Szukiewicz, D. (2014) The role of inflammatory and anti-inflammatory cytokines in the pathogenesis of osteoarthritis. *Mediators Inflamm.* **2014**, 561459, <https://doi.org/10.1155/2014/561459>
- Zhao, J. et al. (2014) Changes of rabbit meniscus influenced by hyaline cartilage injury of osteoarthritis. *Int. J. Clin. Exp. Med.* **7**, 2948–2956
- Scanzello, C.R. and Goldring, S.R. (2012) The role of synovitis in osteoarthritis pathogenesis. *Bone* **51**, 249–257, <https://doi.org/10.1016/j.bone.2012.02.012>
- Tang, J. et al. (2016) Fibroblast growth factor receptor 3 inhibits osteoarthritis progression in the knee joints of adult mice. *Arthritis Rheumatol.* **68**, 2432–2443, <https://doi.org/10.1002/art.39739>
- Lu, J. et al. (2011) MiR-26a inhibits cell growth and tumorigenesis of nasopharyngeal carcinoma through repression of EZH2. *Cancer Res.* **71**, 225–233, <https://doi.org/10.1158/0008-5472.CAN-10-1850>
- Hu, K. et al. (2011) Expression profile of microRNAs in rat hippocampus following lithium-pilocarpine-induced status epilepticus. *Neurosci. Lett.* **488**, 252–257, <https://doi.org/10.1016/j.neulet.2010.11.040>
- Liu, P. et al. (2015) miR-26a suppresses tumour proliferation and metastasis by targeting metadherin in triple negative breast cancer. *Cancer Lett.* **357**, 384–392, <https://doi.org/10.1016/j.canlet.2014.11.050>
- Zhang, Y.F. et al. (2013) MiR-26a regulates cell cycle and anoikis of human esophageal adenocarcinoma cells through Rb1-E2F1 signaling pathway. *Mol. Biol. Rep.* **40**, 1711–1720, <https://doi.org/10.1007/s11033-012-2222-7>
- Sahu, S.K. et al. (2017) MicroRNA 26a (miR-26a)/KLF4 and CREB-C/EBPbeta regulate innate immune signaling, the polarization of macrophages and the trafficking of Mycobacterium tuberculosis to lysosomes during infection. *PLoS Pathog.* **13**, e1006410, <https://doi.org/10.1371/journal.ppat.1006410>
- Yin, X., Wang, J.Q. and Yan, S.Y. (2017) Reduced miR26a and miR26b expression contributes to the pathogenesis of osteoarthritis via the promotion of p65 translocation. *Mol. Med. Rep.* **15**, 551–558, <https://doi.org/10.3892/mmr.2016.6035>
- Wei, C. et al. (2013) NF-kappaB mediated miR-26a regulation in cardiac fibrosis. *J. Cell. Physiol.* **228**, 1433–1442, <https://doi.org/10.1002/jcp.24296>
- Xie, Q. et al. (2015) Reciprocal inhibition between miR-26a and NF-kappaB regulates obesity-related chronic inflammation in chondrocytes. *Biosci. Rep.* **35**, e00204, <https://doi.org/10.1042/BSR20150071>
- Rigoglou, S. and Papavassiliou, A.G. (2013) The NF-kappaB signalling pathway in osteoarthritis. *Int. J. Biochem. Cell Biol.* **45**, 2580–2584, <https://doi.org/10.1016/j.biocel.2013.08.018>
- Roman-Blas, J.A. and Jimenez, S.A. (2006) NF-kappaB as a potential therapeutic target in osteoarthritis and rheumatoid arthritis. *Osteoarthritis Cartil.* **14**, 839–848, <https://doi.org/10.1016/j.joca.2006.04.008>
- Murata, K. et al. (2013) Comprehensive microRNA analysis identifies miR-24 and miR-125a-5p as plasma biomarkers for rheumatoid arthritis. *PLoS ONE* **8**, e69118, <https://doi.org/10.1371/journal.pone.0069118>
- Wu, Y. et al. (2017) CircRNA hsa.circ.0005105 upregulates NAMPT expression and promotes chondrocyte extracellular matrix degradation by sponging miR-26a. *Cell Biol. Int.* **41**, 1283–1289, <https://doi.org/10.1002/cbin.10761>
- Mankin, H.J. et al. (1971) Biochemical and metabolic abnormalities in articular cartilage from osteo-arthritic human hips II. Correlation of morphology with biochemical and metabolic data. *J. Bone Joint Surg. Am.* **53**, 523–537, <https://doi.org/10.2106/00004623-197153030-00009>

- 23 Krenn, V. et al. (2002) Grading of chronic synovitis—a histopathological grading system for molecular and diagnostic pathology. *Pathol. Res. Pract.* **198**, 317–325, <https://doi.org/10.1078/0344-0338-5710261>
- 24 Krenn, V. et al. (2006) Synovitis score: discrimination between chronic low-grade and high-grade synovitis. *Histopathology* **49**, 358–364, <https://doi.org/10.1111/j.1365-2559.2006.02508.x>
- 25 Siebuehr, A.S. et al. (2014) Identification and characterisation of osteoarthritis patients with inflammation derived tissue turnover. *Osteoarthr. Cartil.* **22**, 44–50, <https://doi.org/10.1016/j.joca.2013.10.020>
- 26 Wang-Saegusa, A. et al. (2011) Infiltration of plasma rich in growth factors for osteoarthritis of the knee short-term effects on function and quality of life. *Arch. Orthop. Trauma Surg.* **131**, 311–317, <https://doi.org/10.1007/s00402-010-1167-3>
- 27 Blagojevic, M. et al. (2010) Risk factors for onset of osteoarthritis of the knee in older adults: a systematic review and meta-analysis. *Osteoarthr. Cartil.* **18**, 24–33, <https://doi.org/10.1016/j.joca.2009.08.010>
- 28 Greene, M.A. and Loeser, R.F. (2015) Aging-related inflammation in osteoarthritis. *Osteoarthr. Cartil.* **23**, 1966–1971, <https://doi.org/10.1016/j.joca.2015.01.008>
- 29 Toh, W.S. et al. (2016) Cellular senescence in aging and osteoarthritis. *Acta Orthop.* **87**, 6–14, <https://doi.org/10.1080/17453674.2016.1235087>
- 30 Sun, J. et al. (2016) Plasma miR-26a as a diagnostic biomarker regulates cytokine expression in systemic juvenile idiopathic arthritis. *J. Rheumatol.* **43**, 1607–1614, <https://doi.org/10.3899/jrheum.150593>
- 31 Bowles, R.D. et al. (2014) In vivo luminescence imaging of NF-kappaB activity and serum cytokine levels predict pain sensitivities in a rodent model of osteoarthritis. *Arthritis Rheumatol.* **66**, 637–646, <https://doi.org/10.1002/art.38279>
- 32 Benito, M.J. et al. (2005) Synovial tissue inflammation in early and late osteoarthritis. *Ann. Rheum. Dis.* **64**, 1263–1267, <https://doi.org/10.1136/ard.2004.025270>
- 33 Goldring, S.R. and Goldring, M.B. (2004) The role of cytokines in cartilage matrix degeneration in osteoarthritis. *Clin. Orthop. Relat. Res.* **427**, S27–S36, <https://doi.org/10.1097/01.blo.0000144854.66565.8f>
- 34 Loeser, R.F. (2009) Aging and osteoarthritis: the role of chondrocyte senescence and aging changes in the cartilage matrix. *Osteoarthr. Cartil.* **17**, 971–979, <https://doi.org/10.1016/j.joca.2009.03.002>
- 35 Ludin, A. et al. (2013) Injection of vascular endothelial growth factor into knee joints induces osteoarthritis in mice. *Osteoarthr. Cartil.* **21**, 491–497, <https://doi.org/10.1016/j.joca.2012.12.003>
- 36 Etich, J. et al. (2015) MiR-26a modulates extracellular matrix homeostasis in cartilage. *Matrix Biol.* **43**, 27–34, <https://doi.org/10.1016/j.matbio.2015.02.014>
- 37 Wu, Y. et al. (2015) Overexpression of Sirtuin 6 suppresses cellular senescence and NF-kappaB mediated inflammatory responses in osteoarthritis development. *Sci. Rep.* **5**, 17602, <https://doi.org/10.1038/srep17602>
- 38 Wang, D. et al. (2015) Thymoquinone inhibits IL-1beta-induced inflammation in human osteoarthritis chondrocytes by suppressing NF-kappaB and MAPKs Osteoarthr. Cartil.athway. *Inflammation* **38**, 2235–2241, <https://doi.org/10.1007/s10753-015-0206-1>
- 39 You, C. et al. (2018) Synovial fibroblast-targeting liposomes encapsulating an NF-kappaB-blocking peptide ameliorates zymosan-induced synovial inflammation. *J. Cell. Mol. Med.* **22**, 2449–2457, <https://doi.org/10.1111/jcmm.13549>
- 40 Yin, H. et al. (2005) Vasoactive intestinal peptide ameliorates synovial cell functions of collagen-induced arthritis rats by down-regulating NF-kappaB activity. *Immunol. Invest.* **34**, 153–169, <https://doi.org/10.1081/IMM-55809>
- 41 Feng, M., Xu, D. and Wang, L. (2018) miR-26a inhibits atherosclerosis progression by targeting TRPC3. *Cell Biosci.* **8**, 4, <https://doi.org/10.1186/s13578-018-0203-9>